AIP | Review of Scientific Instruments

Contactless automated manipulation of mesoscale objects using opto-fluidic actuation and visual servoing

Emir Vela, Moustapha Hafez, and Stéphane Régnier

Citation: Review of Scientific Instruments **85**, 055107 (2014); doi: 10.1063/1.4874744
View online: http://dx.doi.org/10.1063/1.4874744
View Table of Contents: http://scitation.aip.org/content/aip/journal/rsi/85/5?ver=pdfcov
Published by the AIP Publishing

Contactless automated manipulation of mesoscale objects using opto-fluidic actuation and visual servoing

Emir Vela,[1,a)] Moustapha Hafez,[2] and Stéphane Régnier[3]
[1]*Department of Mechanical Engineering, Universidad de Ingeniería y Tecnología, Av. Cascanueces 2221 Santa Anita, Lima, Peru*
[2]*CEA LIST, 18 route du Panorama, BP 6, 92265 Fontenay-aux-Roses, France*
[3]*Institut des Systèmes Intelligents et de Robotique, Université Pierre et Marie Curie/CNRS UMR 7222, 4 Place Jussieu, 75005 Paris, France*

(Received 17 October 2013; accepted 22 April 2014; published online 9 May 2014)

This work describes an automated opto-fluidic system for parallel non-contact manipulation of microcomponents. The strong dynamics of laser-driven thermocapillary flows were used to drag microcomponents at high speeds. High-speed flows allowed to manipulate micro-objects in a parallel manner only using a single laser and a mirror scanner. An automated process was implemented using visual servoing with a high-speed camera in order to achieve accurately parallel manipulation. Automated manipulation of two glass beads of 30 up to 300 μm in diameter moving in parallel at speeds in the range of mm/s was demonstrated. © *2014 AIP Publishing LLC*. [http://dx.doi.org/10.1063/1.4874744]

I. INTRODUCTION

The miniaturization of products and systems towards the microscale makes the manipulation and assembling tasks much more complex. New trends in the development and production of microsystems are directed to the (self-)assembly[1–3] of hybrid microcomponents such as MEMS, MOEMS, laser microsources, and organic-based microdevices. However, at this scale the handling of micro-objects is challenging because of the adhesion forces between end-effectors, components, and substrates. In addition, a high throughput is needed in order to assemble microparts in a fast, parallel, and automated manner, thus enabling a cost-effective massive production. There are some non-contact micromanipulation techniques that could be used for this purpose such as optical tweezers,[4,5] electromagnetic tweezers,[6] opto-dielectrophoresis,[7] acoustic waves,[8] and more recently opto-thermocapillary effects,[9,10] and marangoni flow.[11] The mentioned techniques manipulate objects depending on their shape, size, and material composition. For instance, objects manipulated by optical tweezers have to be transparent to light and their shapes have to be approximately a sphere. However, it would be more interesting and would have more impact if a method that achieves manipulation of objects of any shape, size, and composition could be developed. For instance, if an assembly of electronic microcomponents such as LEDs is required, the non-contact method has to deal with the shape and material composition of the LEDs in order to displace them and force their encounter for assembly. In addition, the non-contact manipulation method has to allow automation of the process to achieve multiple and precise object manipulation.

In this work, the automation of a micromanipulation system is presented, which is capable to perform non-contact manipulation of micro-objects in a single/parallel manner. The manipulation method is based on LASER-driven thermocapillary flows due to their strong dynamics, which involves high-speed flows (mm/s range) and fast response time for flow generation.[12] As flows are utilized to drag objects, the objects can be of any shape and material composition, moreover in a wide range size. Thus, objects such as capacitors, resistors, LEDs, biological cells,[13] in fact any kind of micro-objects, can be displaced by the presented system. This system was able to manipulate micro-objects such as glass beads, microcapacitors, silicon cubes in a range size of 8–300 μm at speeds of mm/s range.[14] The manipulation system was fully automated using visual servoing in order to manipulate micro-objects in a single/parallel manner for precision positioning. As results, the automated manipulation of two glass beads is discussed. The presented system could have a strong potential as a scientific instrument for manipulation and study of mesoscale objects regardless of their geometrical shapes, sizes, and material compositions.

II. EXPERIMENTAL SETUP

The system (Fig. 1) was composed of an Olympus inverted microscope IX71, a 4× objective lens (NA = 0.1 and working distance = 18.5 mm). An IR laser beam of 1480 nm in wavelength, 120 mW of maximum power, beam diameter of 3 mm, as the heat source. A 2-DoF tip-tilt electromagnetic mirror scanner addressed, through the objective lens, the laser beam into the sample. A high-speed DALSA Genie Monochrome CMOS camera (1 in., 1400 × 1024 pixels at 60 fps) was used to image and obtain position data for visual servoing. A NI USB-6210 data acquisition card drove the laser system and mirror scanner. A petri dish (soda-lime-glass, 60 mm in diameter and 12 mm in height) was filled with distilled water to a specific depth to create the liquid layer (150–600 μm). The manipulated micro-objects were microcapacitors (300 μm), silicon microparts (100–200 μm), and glass beads ranging from 8 up to 300 μm in diameter.

a)Electronic mail: evela@utec.edu.pe

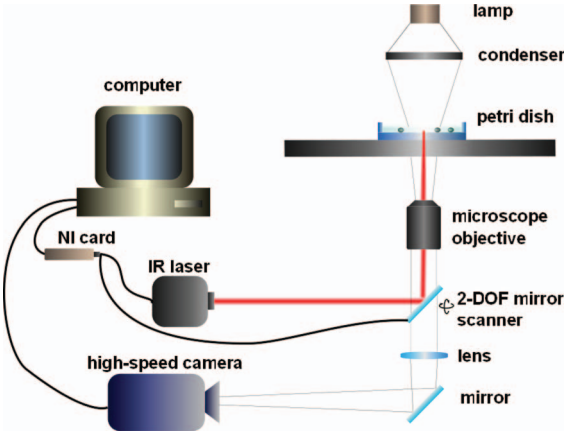

FIG. 1. Schematic of the robotic system. A focused IR laser beam is addressed by a mirror scanner into the sample. A high-speed camera monitored and provided bead positions for visual servoing.

III. RESULTS

The principle used to manipulate micro-objects was the generation of flows in thin water layers by thermocapillary effects. By thermally perturbing the water-air interface of the thin water layer, a shear stress unbalance is produced according to the boundary condition at the interface $\tau = \frac{\partial \sigma}{\partial T}\frac{\partial T}{\partial x} = \eta \frac{\partial u_x}{\partial y}$ where τ is the shear stress, $\frac{\partial \sigma}{\partial T}$ is the temperature derivative of surface tension, $\frac{\partial u_x}{\partial y}$ is the strain rate of the liquid, and η is the viscosity. The shear stress unbalance produces flow generation. To maintain an energy balance of the flows, a recirculation flow is established giving a null overall flow rate, the convection cell used for micromanipulation. To generate a highly localized convection cell an IR Laser beam was used as thermal source in order to perturb the water interface. At this scale inertial effects are highly reduced, in consequence microflows generation could be controlled (Reynolds number is very small for thin liquid layers) by switching on and off the IR laser beam. When the laser beam is switched on, the objects are dragged by the flows, and by switching the laser off the flows are stopped, therefore the objects stop moving. It was observed that by changing the radiation position of the laser beam onto the interface, the convection cell followed the laser position. In other words, the objects inside the convection cell followed the laser beam position. To automatically manipulate beads inside this region it was necessary to estimate the time in which the flows started moving, the exposure time of the laser beam, the water depth and the distance between the laser beam and the glass beads. These parameters had to be implemented in the automated controller. In Fig. 2, the diameter of the convection cell is shown as a function of the exposure time of the laser beam where the water depth was about 150 μm. In 1 s the convection cell reached its maximum diameter (about 2.5 mm), and at 220 ms it reached about 70% of it. At 20 ms, flows started moving. The diameter of the convection cell depends on the water depth. The larger the water depth, the larger the diameter (Fig. 3). On the other hand, the larger the water depth, the smaller the speed of flows.[14] The water depth gives the size of the convection cell, the region where the micro-objects have to be placed according to the laser beam position (centre of the convection cell). The

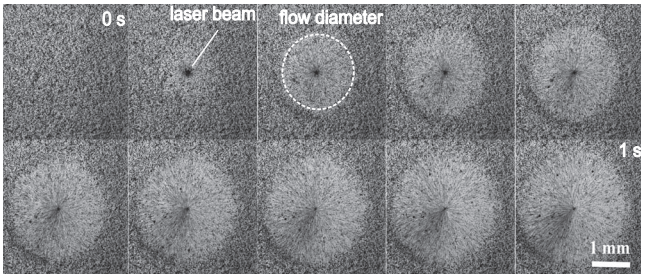

FIG. 2. Diameter of the convection cell depicted by pictures captured every 10 ms (100 Hz with 500 × 500 pixels per image). Images are shown every 110 ms. Hollow glass beads of 8 up to 12 μm in diameter, which density is similar to water, were used as tracers in a depth of water of 150 μm.

distance between the laser beam and the objects gives the speed of the object motion.[14] Moreover, as the laser beam is shot at a specific distance from the micro-objects, the increase in temperature generated by laser absorption of the liquid do not reach them. Thus if the objects are temperature sensitive they are not affected.[12] These parameters were involved in the algorithm developed in this work to perform automated parallel micromanipulation.

IV. ALGORITHM FOR AUTOMATED MICROMANIPULATION

The algorithm was as follows (Fig. 4), beads were detected within the workspace (an area of a petri dish filled with distilled water) using image segmentation in order to capture their image templates. The user then gave the target positions of the beads by clicking with a computer mouse on the displayed video. Image region of interests (ROIs), smaller than the workspace and larger than the beads sizes, were positioned at each bead centre of mass. Then image correlation was computed between the beads templates and the ROIs in order to obtain the bead positions while beads were moving within their respective ROI. A line path vector was calculated between the bead and target position. The laser beam was shot at a distance d from the bead to generate flows and in consequence bead displacements during laser exposure time. Image correlation computed the new bead position. Once this

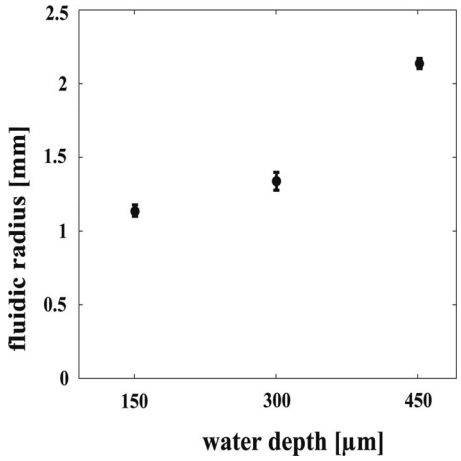

FIG. 3. Radius of the convection cell vs. depth of water. The radius increases with the water depth. Error bars are computed out of five measurements.

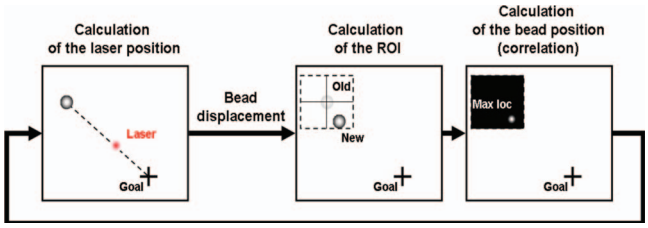

FIG. 4. Schematics of the tracking method using image correlation. The laser is shot at a distance d from the bead to handle it, the bead moves towards the laser beam and then the ROI image updates its position in order to not to lose the future bead position. Once the bead position computed, the laser is shot again at the same distance d. This continues until beads reach their target positions.

obtained, the ROI updated its location in order to have the present bead position at the ROIs centre. For a new bead position, the line path vector was recalculated to address the IR laser beam within this line while keeping the same distance d from the bead. For each iteration, the distance between the bead and target position was compared to a desired position tolerance introduced in the program. When the bead-target position distance was smaller than the position tolerance, the process ended. The highest accuracy that the system could achieve was one pixel, which is the position error given by the image correlation process. In the micromanipulation system presented one pixel corresponded to 5 μm. The time to achieve the displacement of a bead in a closed loop controller was given by the sum of: the laser exposure time (20–90 ms) and the mirror scanner response time (125 ms) that gave 175 ms as a maximum. The image correlation time (2 ms) was not taken into account because it was computed in a parallel thread of the program.

V. DISCUSSION

Experiments were carried out to validate the whole automation process of the presented non-contact parallel manipulation method. The automated manipulation of two glass beads is depicted in Fig. 5, these beads were 50 and 85 μm in diameter, respectively. The water depth was 450 μm that gave with the laser shot distance d, the motion speed of the beads.[14] First of all, the beads were located by the user within an image frame of 500 × 500 pixels Fig. 5(a). One pixel corresponded to 5 μm in the workspace. Then the detection process was started by the user on the graphical user interface (GUI) developed for the system. A detection image filter was implemented to avoid detecting impurities or beads smaller than 30 μm and larger than 150 μm in diameter, these parameters could be changed in the program through the GUI. Once the beads were detected, the user introduced the target positions or destinations by clicking with a computer mouse on the displayed video (Fig. 5(b)). The target positions were highlighted with a black circle of 50 μm in radius. The position tolerance introduced was 10 pixels (50 μm). That meant when the beads centre of mass was located at a distance smaller than 10 pixels from the target position, the automated manipulation process ended. This tolerance could be changed in the program. After the introduction of the target positions, the laser beam was shot at a distance of 450 μm (it corresponded to 90 pixels) from each bead during 90 ms of exposure time (Fig. 5(c)). The laser position was switched from one bead position to the other in order to move each bead by one step after the other during 90 ms (Figs. 5(c)–5(h)). This strategy was implemented due to the radial or toroidal shape of flows that could influence the displacement of both beads at the same time. Due to the different distance destinations, one of the two beads arrived to its destination faster (Fig. 5(g)). As a result, the laser beam was focused on the remaining bead until it reached its final position. When the two beads were in their respective target positions the automated process stopped. The pictures in Figs. 5(c)–5(h) are shown at an interval of 1 s, taking a time of 6 s, since the user introduced the goal positions for both beads to reach their destinations. The image frames were captured at 80 Hz, at this acquisition frequency the bead positions were not lost while moving and performing image correlation between beads templates and ROIs. The position accuracy was smaller than 10 pixels, it depended on the implemented algorithm controller (PI in this case). However, it could be improved by implementing a more suitable controller in order to reach an accuracy of 1 pixel. Besides, the manipulation process could be reconfigurable according to the required manipulation, for example, flows can be engineered by changing the pattern of the laser beam radiation such as circles, lines, multiple dots or other specific geometry, the whole process in an automated manner. This strategy was designed because of the nature of the convection cell, for that reason the laser beam was shot from one bead to another to avoid the effect of the convection cell of one bead to the other

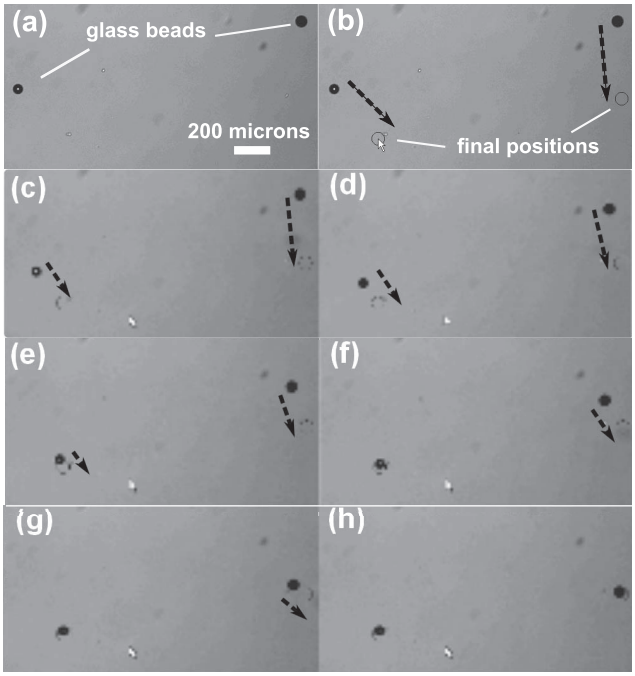

FIG. 5. Image sequence depicting the automated parallel manipulation of two beads. (a) The bead positions were detected by image segmentation in the program. (b) The user introduces the respective target positions with a computer mouse by only clicking on the video. (c)–(h) The IR laser beam was shot by switching from one bead position to the other until the beads reached their destinations. Black arrows represent vector paths from bead to target positions. The pictures are shown at intervals of 1 s. Scale bar of 200 μm. (Multimedia view) [URL: http://dx.doi.org/10.1063/1.4874744.1].

one. It means if both beads were inside the same convection cell they moved to the same target position. This can also be improved by changing the algorithm controller.

VI. CONCLUSION

The opto-fluidic manipulation system presented in this work could open interesting ways to contactless manipulate micro-objects in a fast and parallel manner regardless of their material composition, geometrical shape and in addition with dimensions within a large range size. The system was based on the generation of localized thermocapillary flows in order to drag objects in the direction of flows. As the flows presented negligible inertial effects, the displacements of micro-objects were predictable, thus enabling the design of a controller for manipulate them automatically. An algorithm controller was implemented in order to fully automate the proposed manipulation system, it succeeded to automatically manipulate in parallel two glass beads with different sizes and place them in desired target positions. The position accuracy was smaller than 10 pixel, however it can be improved by developing a more suitable controller.

This system could be interesting for the transport and (self)assembly of micro-components, and even the manipulation of biological cells such as ovocytes in order to study their behavior. Even if micro-objects were temperature sensitive and the manipulation method is based on temperature effects, the micro-objects are protected from temperature effects because they are placed at specific distances from the laser beam radiation where the temperature is higher.

ACKNOWLEDGMENTS

These investigations were supported by the European GOLEM project, Bio-inspired Assembly Process for Mesoscale Products and Systems, FP 6, NMP, Contract No. STRP 033211. The authors acknowledge OCTAX Microscience GmbH for providing the laser shot system and for helpful discussions on the laser-liquid medium interactions.

[1]N. Bowden, F. Arias, T. Deng, and G. M. Whitesides, Langmuir **17**, 1757 (2001).
[2]H. Onoe, K. Matsumoto, and I. Shimoyama, Small **3**, 1383 (2007).
[3]J.-H. Cho, A. Azam, and D. H. Gracias, Langmuir **26**, 16534 (2010).
[4]F. Arai, K. Onda, R. Iitsuka, and H. Maruyama, in *Proceedings of IEEE International Conference on Robotics and Automation (ICRA)* (IEEE, 2009), p. 1832.
[5]P. Rodrigo, R. Eriksen, V. Daria, and J. Glueckstad, Opt. Exp. **10**, 1550 (2002).
[6]L. Zhang, J. J. Abbott, L. Dong, B. E. Kratochvil, D. Bell, and B. J. Nelson, Appl. Phys. Lett. **94**, 064107 (2009).
[7]P. Y. Chiou, A. T. Ohta, and M. C. Wu, Nature (London) **436**, 370 (2005).
[8]S. Oberti, D. Möller, A. Neild, J. Dual, F. Beyeler, B. Nelson, and S. Gutmann, Ultrasonics **50**, 247 (2010).
[9]D. Baigl, "Photo-actuation of liquids for light-driven microfluidics: State of the art and perspectives," Lab Chip **12**, 3637 (2012).
[10]M. L. Cordero, D. R. Burnham, C. N. Baroud, and D. McGloin, Appl. Phys. Lett. **93**, 034107 (2008).
[11]A. S. Basu and Y. B. Gianchandani, J. Microelectromech. Syst. **18**, 1163 (2009).
[12]E. Vela, C. Pacoret, S. Bouchigny, S. Régnier, K. Rink, and A. Bergander, in *Proceedings of IEEE/RSJ International Conference on Intelligent Robots and Systems (IROS)* (IEEE, 2008), p. 913.
[13]M. Hagiwara, T. Kawahara, and F. Arai, Appl. Phys. Lett. **101**, 074102 (2012).
[14]E. Vela, M. Hafez, and S. Régnier, Int. J. Optomechatronics **3**, 289 (2009).